Society For Biomaterials

Coaxial electrospinning of P(LLA-CL)/heparin biodegradable polymer nanofibers: potential vascular graft for substitution of femoral artery

Wei Zhai,[1] Li-jun Qiu,[2] Xiu-mei Mo,[2] Sheng Wang,[3] Yun-fei Xu,[1] Bo Peng,[1] Min Liu,[1] Jun-hua Huang,[1] Guang-chun Wang,[1] Jun-hua Zheng[1]*

[1]Department of Urology, Shanghai Tenth People's Hospital, Tongji University School of Medicine, Shanghai, 200072, China
[2]Institute of Biological Engineering, Donghua University, Shanghai, 201620, China
[3]Department of Intensive Care Unit, Shanghai Tenth People's Hospital, Tongji University School of Medicine, Shanghai, 200072, China

Received 12 November 2012; revised 28 March 2013; accepted 21 April 2013
Published online 7 June 2013 in Wiley Online Library (wileyonlinelibrary.com). DOI: 10.1002/jbm.b.32972

Abstract: Electrospinning is one of the most simple and effective methods to prepare polymer fibers with the diameters ranging from nanometer to several micrometers. Poly (L-lactide)-co-poly (ε-caprolactone) (P(LLA-CL)) fibers and P(LLA-CL)/heparin coaxial composite fibers herein were successfully prepared by single electrospinning and coaxial electrospinning, respectively. The prepared endothelialized P(LLA-CL) and P(LLA-CL)/heparin vascular grafts were used in the Beagle dogs experiment to evaluate the feasibility of thus made different scaffolds for substitution of dog femoral artery in early period, medium term, and long term, meanwhile the pure P(LLA-CL) vascular graft was used as the control group during all the experiments. The animal model was established by using the graft materials to anastomose both femoral arteries of dogs. The vascular grafts patency rates (i.e., the unobstructed capacity of blood vessel) were detected by color Doppler flow imaging technology and digital subtraction angiography. To observe the histological morphology at different periods, the vascular grafts were removed after 7, 14, and 30 days, and the corresponding histological changes were evaluated by hematoxylin and eosin staining. The experimental results show that in the early period, the patency rates of pure P(LLA-CL) graft, endothelial P(LLA-CL) graft, and P(LLA-CL)/heparin graft were 75%, 75%, and 100%, respectively; in the medium term, the patency rates of pure P(LLA-CL) graft and endothelial P(LLA-CL) graft were 25%, whereas that of P(LLA-CL)/heparin graft was 50%; the patency rates of pure P(LLA-CL) graft and endothelial P(LLA-CL) graft were down to 0%, whereas the patency rate of P(LLA-CL)/heparin graft was 25% in the long term. This preliminary study has demonstrated that P(LLA-CL)/heparin coaxial composite fiber maybe a reliable artificial graft for the replacement of femoral artery. © 2013 Wiley Periodicals, Inc. J Biomed Mater Res Part B: Appl Biomater 107B: 471–478, 2019.

Key Words: small-diameter vascular grafts, core-shell P(LLA-CL)/heparin fiber, dog model, femoral artery

How to cite this article: Zhai W,Xu Y,Liu M,Zheng J. 2019. Coaxial electrospinning of P(LLA-CL)/heparin biodegradable polymer nanofibers: potential vascular graft for substitution of femoral artery. J Biomed Mater Res Part B 2019:107B:471–478.

INTRODUCTION

Cardiovascular disease is the leading cause of death and disability in Western countries,[1] which often requires vascular reconstruction. Autologous arteries or veins are the most commonly used substitutes for vessel reconstruction in coronary and peripheral bypass procedures. However, autologous vessel is not available for one-third of patients because of preexisting vascular disease, vein stripping, or vein harvesting for previous surgery. To solve these existing problems, many synthetic materials have been used in vascular tissue engineering; however, synthetic materials such as polyethylene terephthalate (Dacron), expanded polytetrafluoroethylene, and polyurethane[2–5] work well for large-diameter vessels, but are not feasible options for grafts smaller than 6 mm in diameter, because they have high risk of thrombosis and infection, limited durability, and lack of compliance.[2] Recently, due to good biocompatibility and as also can be replaced by autologous blood vessel cells and extracellular cell matrix in suitable time, many biodegradable synthetic or natural materials are considered into the research area as potential prosthetic materials such as polyglycolic acid,[3] poly(L-lactic acid) (PLLA),[4] poly(L-lactide)-co-poly (ε-caprolactone) (P(LLA-CL)),[6–8] natural collagen gel, and fibrin gels.[5] Synthetic material P(LLA-CL) is a block copolymer of PLLA and PCL, which has hydrophobicity, good mechanical property, especially the degradation rate, and elastic property that can be controlled by adjusting different ratios of PLLA and PCL, making P(LLA-CL) widely used in tissue engineering field.[6]

For overcoming the thrombosis, occlusion, and long-term patency rates after surgery in small-diameter vascular

Correspondence to: J. Zheng (e-mail: junhuazhenghua@hotmail.com)

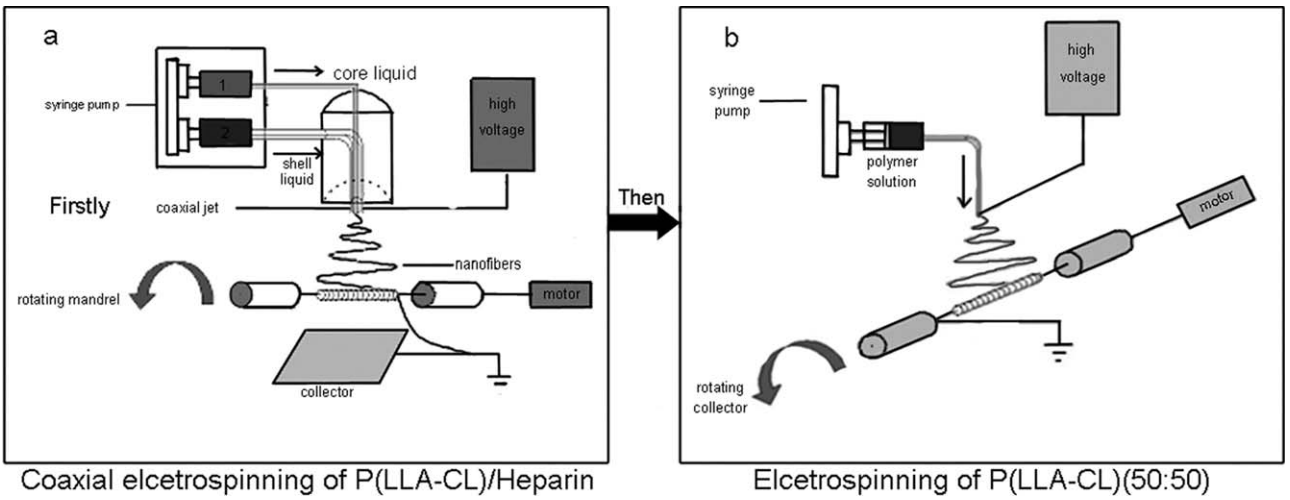

FIGURE 1. Schematic setups of simple (a) and coaxial (b) electrospinning process.

grafts application, preendothelialization of the grafts has been proposed as a method to improve the blood compatibility and optimize the nonthrombosis surface characteristics.[9] However, this technology requires enough effective cell donor, long cell culture time,[10] and hard to avoid the new trauma. So, it is very necessary to prepare well-functionalized artificial prosthesis for overcoming these problems.

In the previous studies, heparin has been used widely as anticoagulant due to its specificity, low collateral responses, and good tolerance by the organism; it also can enhance the proliferation of endothelial cell[6,11] and inhibit the proliferation of vascular smooth muscle cells both *in vivo*[7] and *in vitro*.[8] In vascular graft replacement surgery, to obtain heparin local unremitting release to the site of artificial prosthesis in a long time for reducing coagulant, inhibiting intimal hyperplasia and stenosis, and enhancing the epithelial cells adherence is still a challenge. For the controlled release of heparin, many researches have been done, such as heparin-loaded microcapsules sequestered in a calcium alginate membrane as grafted blood vessel wraps[12] and co-electrospun nanofiber fabric of P(LLA-CL) with heparin as the inner layer.[13] Previous work showed that coaxial electrospinning was a feasible and effective method for fabricating heparin encapsulated and sustained releasing core-shell structural nanofibers.[14]

In this study, copolymer P(LLA-CL) with L-lactide to e-caprolactone ratio of 50:50 was successfully electrospun into pure nanofibers and with heparin-loaded core-shell structural fibers by electrospinning and coaxial electrospinning, respectively. P(LLA-CL)/heparin composite fibers were prepared by using heparin as the core component, while P(LLA-CL) as the shell component. The P(LLA-CL)/heparin grafts were implanted into the femoral arteries of the dogs, taking autogenous preendothelialization and pure P(LLA-CL) fibers grafts as controls. We hypothesized that the controlled and persistent heparin releasing would enhance the self-endothelium by the migration of autogenous epithelial cells from junction sites of the graft with native blood vessel or capture the endothelial progenitor cells from peripheral blood, thus avoiding early thrombosis and improving the long-term patency rates. Thus, it is believed that made heparin-functionalized P(LLA-CL)/heparin core/shell structural composite fiber graft will have potential applications in biomedical fields.

EXPERIMENTAL SECTION

Fabrication of P(LLA-CL) fiber and P(LLA-CL)/heparin composite fiber tubular scaffolds

According to the previous study,[15] 6% w/v P(LLA-CL) (LLA/CL: 50/50, Nara Medical University, Japan) electrospun solution was prepared by dissolving 0.6 g P(LLA-CL) in 10 mL 2, 2, 2-trifluoromethyl ethanol (Dupont company, USA) and stirred on a magnetic stirrer until a transparent solution obtained. The following process parameters were adopted when fabricating single P(LLA-CL) material tubular scaffold: The electrospun solution was placed in a 2.5-mL plastic syringe fitted with a needle of about 0.8 mm diameter. The nano/microfibers were fabricated using electrospinning at 16 kV by using a high voltage power supply (BGG6-358, BMEI CO. LTD, China). The solution was fed into the needle using a syringe pump (789100C, cole-pamer, America), and the feeding rate was fixed at 1.2 mL/h; meanwhile, the rotating speed of the stainless steel bar (collector), the surface of which was covered by a thin aluminum foil, was fixed at 800 rpm/h, and the vertical distance between the collector and the needle tip was fixed at 15 cm. The schematic setup of single electrospinning was illuminated in Figure 1(a).

To obtain coaxial electrospun fiber that loaded heparin as the inner section of the vascular graft, coaxial electrospinning method was performed [Figure 1(b). Six percent P(LLA-CL) was used as the shell material and 12% heparin (13 kDa, Runjie Medicine Chemical, China) dissolved in ultra pure water was used as the core material. During the coaxial electrospinning process, two syringe pumps were used; the feeding rates of the core and shell electrospun

solutions were 0.1 and 1.0 mL/h, respectively. The working voltage, collecting distance, and the rotating speed of collector were same as single P(LLA-CL) electrospinning process. After about 3.5-h single electrospinning of P(LLA-CL) fiber, turn to 1.5-h coxial electrospinning of P(LLA-CL)/heparin composite fiber (Figure 1).

Characterization of electrospun P(LLA-CL) tubular scaffold

The morphology of electrospun fiber tubular scaffolds was investigated through scanning electronic microscopy (SEM; JEOL, JSM-5600, Japan) operated at an acceleration voltage of 8–10 kV. Before SEM measurement, the samples were sputter coated for about 50 s with gold to increase the conductivity. Based on the SEM images, the average diameter of electrospun fibers were measured by using Image J software (National Institutes of Health, USA), and the frequency for diameter measurement were no less than 100.

Meanwhile, the core/shell structure of electrospun P(LLA-CL)/heparin composite fibers was observed by transmission electron microscope (TEM; Hitachi, HitachiH-800, Japan). The samples for TEM measurement were prepared by collecting some single composite fibers onto the surface of carbon-coated copper grid directly and dried in the vacuum oven to evaporate the residual solvent completely before TEM observation.

A universal materials tester (H5K-S, Hounsfield, UK) with a load cell of 50 N and elongation speed of 10 mm/min was used for the mechanical properties testing. All the test process was carried out at ambient temperature $\sim$25°C and relative humidity about 65%.[16] Before testing, the average thickness of tubular scaffold specimens were measured by a micrometer, then cut into 5 cm length $\times$ 1 cm width, and the effective tensile test length was 3 cm. No less than five specimens were tensile test to calculate the average values and standard deviations of the mechanical properties.

Heparin release in coaxial electrospun fiber was tested as following: The coaxial electrospun P(LLA-CL)/heparin mats (20 mm $\times$ 20 mm, approximately 0.062 g) were immersed in phosphate-buffered saline (PBS; 4 mL, pH 7.4) at 37°C. Two microliters of the solution was replaced with a fresh one according to the predetermined schedule: every day in the first week, followed by every 2 days in the next week. The replaced heparin solution (2 mL) was added to the toluidine blue solution (0.005% in 0.01 N HCl containing 0.2% NaCl, 3 mL), and the mixed solution was adequately vibrated and then reacted at 37°C for 2 h. After that, hexane (3 mL) was added, and the mixture was well shaken to make sure that the toluidine blue–heparin complex was adequately extracted into the organic layer. After that, the absorbance of the aqueous phase was measured by ELIASA at 630 nm.

Endothelialization of P(LLA-CL) vascular graft

Endothelial cells were obtained from the autogenous femoral veins (about 6–10 cm length) of dogs by the method of trypsin digestion. The detail method was performed as following: the femoral vein was washed three times using PBS; the femoral vein was applied in an in site cannulation technique so as to avoid endothelial cells being contained and filled with 0.25% trypsin solution (Gibco, USA) for 5 min in a cell incubator. The suspension was washed down by high sugar Dulbecco's modified Eagle medium (DMEM) into a 15-cm centrifuge tube. After centrifugation at 1000 rpm at 4°C for 8 min, the cells were resuspended with high sugar DMEM supplemented with 10% fetal bovine serum and cultured for nearly 3 weeks. The endothelial cells suspensions were seeded into the P(LLA-CL) vascular graft at cell density of 1×10^2/mL for four times. After the first seeding for 2 h, the vascular graft was rotated by 90° to perform the second seeding. The graft was moved into a culture dish with a diameter of 10 cm cultivated for 2 weeks. A 5-cm endothelialized vascular graft was cut for implantation, and the other section was fixed in 4% glutaraldehyde solution for observing the morphology by SEM.

Implantation of the scaffolds into dog model

Eight Beagle dogs weighting 15–20 kg were anesthetized by intravenous injecting of sodium pentobarbital (30 mg/kg) and then randomly divided into two groups: four dogs for endothelialized P(LLA-CL) vascular graft implantation (group A) and the other four dogs for P(LLA-CL)/heparin vascular graft implantation (group B), and all the dogs received the pure P(LLA-CL) scaffolds as self-control (group C). A bilateral femoral arteries implant model was applied in this study. With the dogs were supined, right incision was made on the right and left legs, 3-cm segments of the femoral arteries were removed bilaterally while the arteries were clamped. The pretreated 5-cm length vascular grafts were inserted the middle with 7-0 Prolene sutures. The incision sites were sealed carefully with 10-0 sutures. All the dogs were intramuscularly injected with penicillin (800,000 U) and given Warevan tablet for 3 consecutive days after the surgery. From the fourth day, the dogs were given only Warevan tablet until the vascular grafts were removed. During this process, we observed the activity, pulsatility, and operative incision of dog lower limbs. Vascular graft patency rate was detected by color Doppler flow imaging technology (CDF) and digital subtraction angiography (DSA). The vascular grafts including the proximal, the middle, and the distal end were removed after 7, 14, and 30 days, and the corresponding histological changes were evaluated by hematoxylin and eosin (HE) staining.

RESULTS

Morphology observation of P(LLA-CL) and P(LLA-CL)/heparin fiber vascular graft

As shown in SEM micrographs in Figure 2(a,b), smooth surface and uniformity diameter distribution of P(LLA-CL) and P(LLA-CL)/heparin fibers have been obtained. The elecrtrospun P(LLA-CL)/heparin fibers were combined together at the place of fibers stacking as same as the electrospun P(LLA-CL). Those nodes may be able to strengthen the mechanical properties. The P(LLA-CL)/heparin coaxial electrospun fibers as the inner layer of vascular graft can be clearly seen in the SEM micrograph [Figure 2(c)], in the

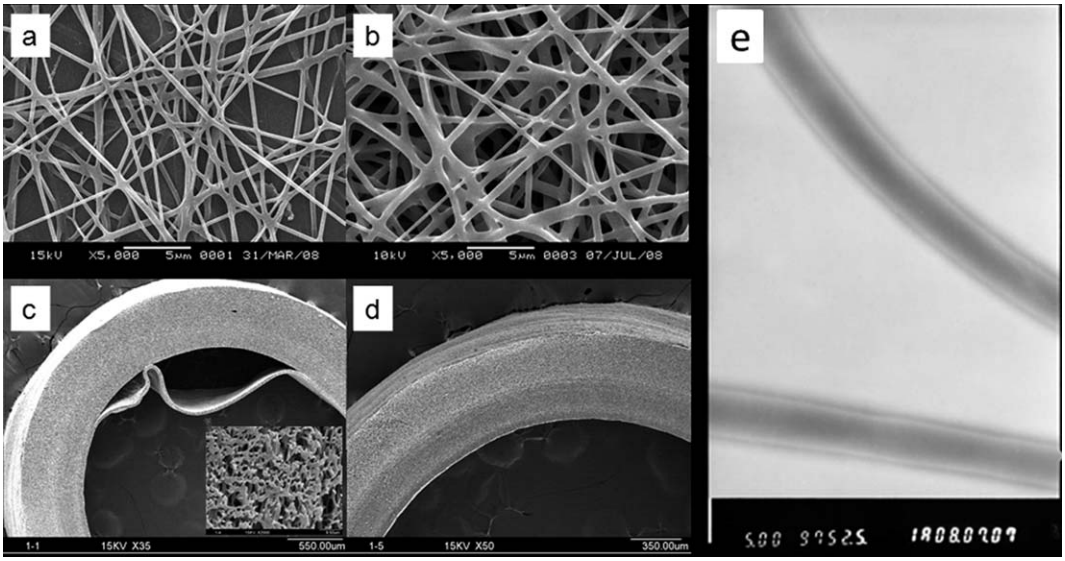

FIGURE 2. SEM and TEM micrographs of P(LLA-CL) and P (LLA-CL)/heparin fibers and vascular graft: (a) P(LLA-CL)/heparin coaxial electrospun fibers, (b) P(LLA-CL) electrospun fibers, (c) the cross-section of graft contains P(LLA-CL)/heparin coaxial fibers as the inner, (d) the cross-section of graft without P(LLA-CL)/heparin coaxial fibers inner, and (e) TEM micrographs of P(LLA-CL)/heparin coaxial electrospun fibers.

lower right corner of Figure 2(c), a magnification micrograph of the cross-section of the scaffold shows a well-distributing porosity vascular graft structure, which may enhance the cell nutrients penetrate and the smooth muscle cells grow into the graft, and benefit for the reconstruction of new blood vessel. In addition, an obvious core-shell structure of electrospun P(LLA-CL)/heparin can be identified in TEM image [Figure 2(e)]. The anticoagulant heparin as the core layer was encapsualted perfectly by P(LLA-CL), and the coaxial fibers have good continuity (Figure 2).

Mechanical properties of P(LLA-CL) and P(LLA-CL)/heparin fiber vascular graft

From Figure 3, it is clearly seen that the P(LLA-CL) and P(LLA-CL)/heparin vascular grafts have a good mechanical properties no matter under dry or wet conditions. As for P(LLA-CL) vascular graft, the tensile stress and strain in the wet condition could reach 21.25 ± 0.35 MPa and $516 \pm 19.84\%$, respectively, whereas under dry condition, the tensile stress and strain were 18.34 ± 0.18 MPa and $504 \pm 21.62\%$, respectively. As for P(LLA-CL)/heparin vascular graft, the tensile stress and strain under dry condition were 17.56 ± 0.43 MPa and $460 \pm 33.14\%$, respectively. Although slightly reduced compared with the pure P(LLA-CL) graft, the mechanical property of P(LLA-CL)/heparin vascular graft can still meet the demand for artificial vascular graft (Figure 3).

Heparin *in vitro* release study

As shown in Figure 4, the cumulative release of heparin had reached 68% in the first week, but subsequently the release rate was gradually lower, and it only reached 72% until the

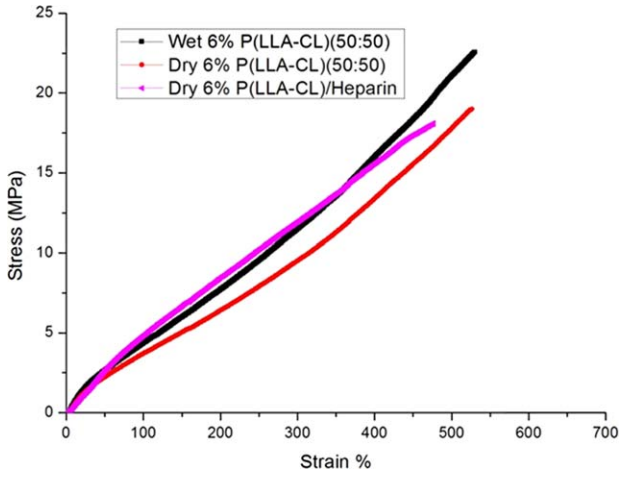

FIGURE 3. Typical stress-strain curves of prepared P(LLA-CL) graft at wet and dry conditions and P(LLA-CL)/heparin graft at dry condition.

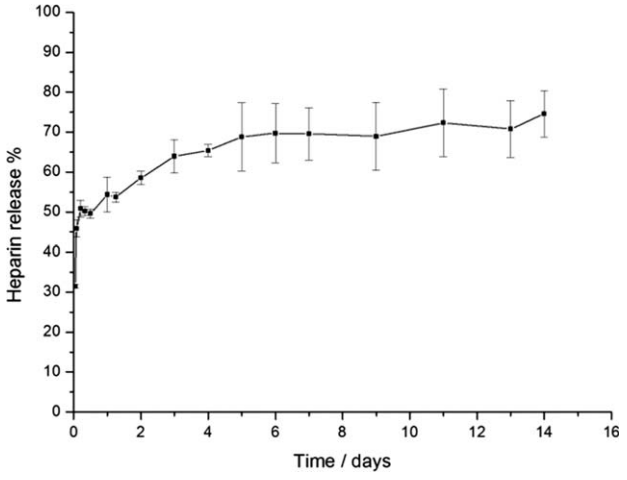

FIGURE 4. The release curve of 12% heparin in coaxial P(LLA-CL) (50:50)/heparin core/shell composite fibers.

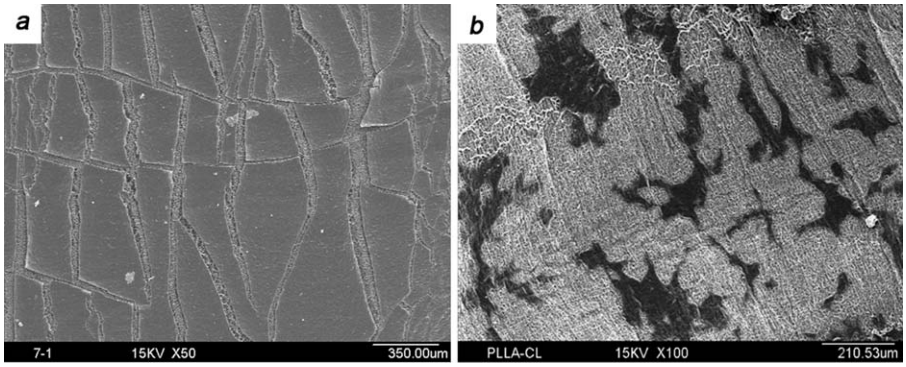

FIGURE 5. Endothelialization of P(LLA-CL) fibers: (a) 1 week and (b) 2 weeks.

14th day. We consider that the heparin release is mainly completed through two ends of core/shell fiber and the heparin is water-soluble medicine; therefore, the release rate was higher in the first week. However, the siphon release and cortex penetration were major release manner, resulting in a lower release rate of heparin in the following weeks (Figure 4).

Endothelialization of P(LLA-CL) vascular graft

The morphology of the endothelialized P(LLA-CL) cultivated in 1 week and 2 weeks were shown in Figure 5(a,b), respectively. From the images, it is clear that the inner surface of the scaffold has been covered by canine femoral artery endothelium, and this coating has a certain thickness. The endothelialized P(LLA-CL) fiber was used as one of the scaffolds for vascular graft implantation (Figure 5).

The basic activity, pulsatility, and operative incision after vascular graft implantation

Eight dogs survived after vascular graft implantation. The pulsatilities in both lower limbs of eight dogs were good. They could stand and walk freely. There was no significant local tissue inflammation in operative incision, such as swelling and diabrosis.

Patency rate after vascular graft implantation

The patency rates of endothelialized P(LLA-CL) (group A), P(LLA-CL)/heparin (group B) and pure P(LLA-CL) (group C) graft groups were 75%, 100%, and 75%, respectively, in the early stage. In the medium term, the patency rate of group A and group C was 25%, whereas that of group B was 50%. In the long term, the patency rates of group A and group C was 0%, whereas that of group B was 25%. From Table I, it can be seen that the patency rate of group B was higher than that of group A and group C (Table I).

TABLE I. The Patency Rates of Three Vascular Grafts

Group	Early Stage (3–7 d)	Medium Term (14–21 d)	Long Term (30 d)
A	3 (75%)	1 (25%)	0 (0%)
B	4 (100%)	2 (50%)	1 (25%)
C	6 (75%)	2 (25%)	0 (0%)
p	>0.05	>0.05	>0.05

A, Endothelialized P(LLA-CL) vascular graft implantation; B, P(LLA-CL)/heparin vascular graft implantation; C, pure P(LLA-CL) scaffolds as self-controls.

Histopathological observation after vascular graft implantation

Compared with the preoperation, visual study indicated there were no shape and elasticity change, as well as no degradation in these three vascular grafts 7 days after the implantation. However, spindle red thrombus, rough, uneven intima, and anastomotic stenosis were observed 30 days after vascular graft implantation in group A and C. But no calcification and stenosis were present in the anastomosis of group B, only with a slight thickening.

Furthermore, the histopathological changes were observed under microscope according to HE staining. The results revealed that 30 days after endothelialized P(LLA-CL) vascular graft implantation, the vascular shape was still clear, but there was a jagged profile in the inner and outer layers of vascular graft, suggesting some structural degradations[Figure 6(a1-c1)]. Blue staining in the inner surface of vascular graft demonstrated that there was a layer of endothelial cell adhesion to the inner surface of vascular graft. However, their incoherent and uneven distribution explained a lower degree of endothelialization.[17] In addition, Figure 6c1 indicated there was some thrombus in the distal intracavity.

As for the P(LLA-CL)/heparin vascular graft, endothelial cell coverage decreased progressively from the proximal to the distal end of vascular graft 30 days after implantation [Figure 6(a2-c2)], indicating a proliferation and migration process. There was some degradation in the outer layer of the proximal end, and some endothelial cells adhere to the outer layer of vascular graft. However, no significant thrombus and inflammation were observed. Figure 6(d1-f1, d2-f2) showed the histopathological changes of pure P(LLA-CL) vascular graft. From the results, it can be seen that there was clear red mass in the core of vascular graft [Figure 6(d1-f1)], indicating

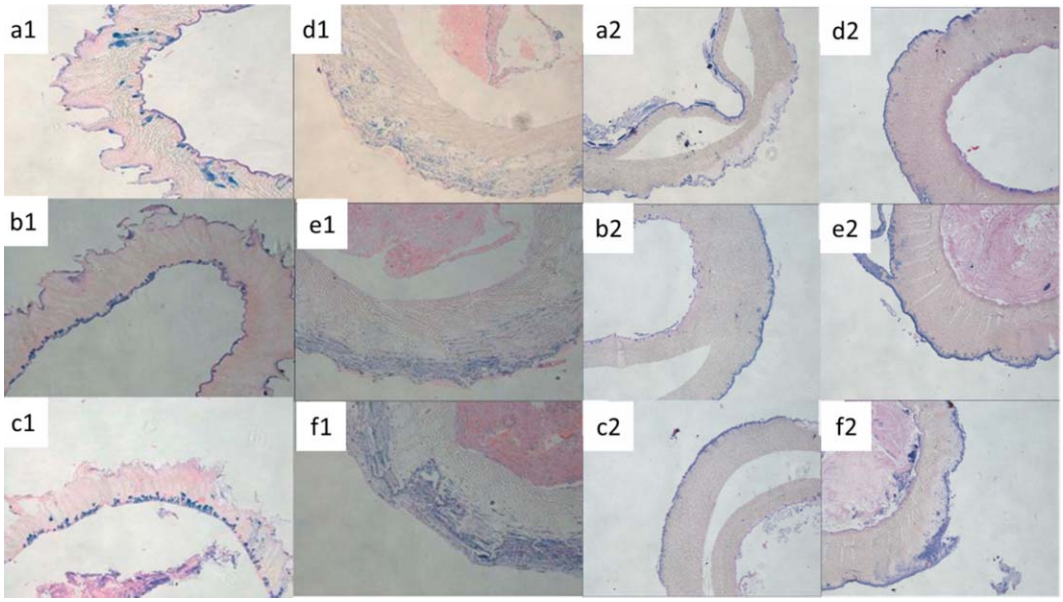

FIGURE 6. The HE micrographs of endothelialized P(LLA-CL), P(LLA-CL)/heparin, and pure P(LLA-CL) vascular grafts implantation for 30 days: (a1–c1) the proximal end, the middle, and the distal end of endothelialized P(LLA-CL) vascular graft, (a2c2) the proximal end, the middle, and the distal end of P(LLA-CL)/heparin vascular graft, and (d1–f1) and (d2–f2) the proximal end, the middle, and the distal end of pure P(LLA-CL) vascular graft.

significant thrombus occurred in the proximal, middle, and distal end (Figure 6).

DISCUSSION

The search for ideal vascular substitute grafts for cardiovascular applications has far been half a century endeavor. Although successfully used for large and medium blood vessel replacement, synthetic vascular grafts have never been proved successful in small-diameter blood vessel (inner diameter <6 mm) replacement due to the existing of thrombosis, stenosis, and occlusion.[18] Therefore, finding a solution for small-diameter bypass grafting has recently become a major focus of attention.

The synthetic material selection is one of the most crucial factors for long-term patency rate.[19] After implantation, traditional nondegradable polymer materials can be permanently accumulated in human body, which can stimulate intimal hyperplasia and thrombopoiesis, especially in the anastomosis. Therefore, these materials are not suitable as substitute small-diameter blood vessels to popularize in clinic.[20] Biodegradable polymer materials have several advantages, for example, we could predesign and regulate their mechanical properties, degradation rate, and time; they can be degraded into small molecules for some time and replaced by new tissues *in vivo,* resulting in few adverse reaction; it also possess perfect plasticity, low antigenicity, and good compatibility.[21] Several studies have demonstrated that P(LLA-CL) small-diameter blood vessel has excellent physicochemical, mechanical, and biodegradable properties, and cells could grow well in P(LLA-CL) membrane.[15,22] In this study, we implanted P(LLA-CL) vascular graft into dog model and found that there was no significant side effect after 9 months, indicating good compatibility of the P(LLA-CL) vascular graft.

Electrostatic spinning, or electrospinning, is an attractive approach for the production of much smaller diameter fibers in which a stream of a polymer solution or melt is subjected to a high electric field force.[23,24] The obtained small-diameter tubular scaffold possess high specific surface area, porosity, and interconnected three-dimensional network structure, therefore can better mimic natural blood vessels skeleton structure compared with the tubular scaffold prepared by conventional methods.

We selected Beagle dogs as animal model because the diameter of canine vascular is larger than that of rabbit, thus allowing easy and precise reconstruction of vascular anastomosis. As we expected, eight dogs were all survived, could stand, and walk freely early after vascular graft implantation, indicating well blood patency. Furthermore, CDF and DSA analyses also indicated that in the early stage, the patency rates of endothelialized P(LLA-CL) (group A), P(LLA-CL)/heparin (group B), and pure P(LLA-CL) (group C) groups were 75%, 100%, and 75%, respectively. These findings indicated that implantation within 7 days can ensure higher patency rate. There was a similar patency rate between group A and group C vascular grafts in the early stage (75%), suggesting the endothelialization could not improve the patency rate. We predicted that it maybe because of a low degree of endothelialization in our study and therefore did not play an effective role in antithrombosis. The poor endothelialization may be caused by the following causes: (1) limited primary vascular endothelial cells in dog model and lower cell division rate, resulting in lower cell concentration; (2) some endothelial cells were scraped during the process of washing the femoral vein; and (3)

some faults in the cultivation methods and instruments, leading to suppressive endothelial cells growth and adhesion to the inner surface of blood vessel prosthesis.

In the medium term, the patency rates of group A and group C were 25%, whereas that of group B was 50%. In the long term, the patency rates of group A and group C were 0%, whereas that of group B was 25%. These results suggested that the patency rates of these three groups were all gradually decreased along from 7 to 30 days, which may result from the following causes: (1) Different degree of vascular intima damage. The integrity of vascular intima is an important factor to maintain antithrombotic effect. It not only prevents the contact between blood and other tissues of vascular wall but also produces the vascular activator to inhibit platelet adhesion aggregation.[25] Impaired vascular intima stimulates the coagulation system and cause thrombosis. (2) The small diameter leads to relative lower blood flow rate.[26] Therefore, the platelets are easily deposited in the inner surface of vascular prosthesis and causes stenosis or even blockages. (3) An inconsistent vascular and autologous femoral artery diameter.[27] Although vascular prosthesis was 2.5–3.5 mm in diameter, which meets the criterion of diameter $<$6 mm, this small diameter could lead to stenosis in anastomosis. (4) Poor endothelialization leads to platelet adhesion and aggregation.[28,29] (5) High coagulation of dog blood and dosage control of anticoagulation drugs are also one of the causes. [30,31] The oral absorptivity of warfarin is 100%, and the blood concentration reaches the peak after 60–90 min. Its anticoagulation effect emerges 2–7 days after treatment, and the therapeutic concentration range could be controlled according to the international normalized ratio of 2.0–3.0.[32] However, the drug control was not performed in this study, and thus, the low dose can cause thrombus.

Importantly, the patency rates of group C and group A vascular graft were lower than that of group B vascular graft. These suggest the heparin could be slowly released during implantation process and thus effectively prevent thrombopoiesis. According to the results of controlled release curve, we could find that the heparin release was 68% at the first week and thus effectively prevent thrombopoiesis. However, the heparin release was lower after 1 week, leading to a reduced patency rate. In brief, the patency rate of P(LLA-CL)/heparin vascular graft is superior to two others at the long-term period. If vascular graft can maintain long-term patency rate in animal model, there are reasons to believe that this artificial material is a potential alternative in clinical application.

Based on the mechanism of HE staining, cells were shown bluish violet; extracellular matrix and red blood cells or protein liquids were shown in red and pink, respectively. In this study, we found that there was a layer of endothelial cells covered in the inner surface of vascular graft, and some blue cells were gradually migrated into the medium of blood vessel prosthesis. These results suggested that P(LLA-CL) vascular graft fabricated by electrospinning had certain porosity, making vascular fibroblasts and smooth muscle cells migrate into the blood vessel prosthesis, replacing the degradative blood vessel prosthesis via cell growth, proliferation, and secretion. There was no calcification in the adventitia, significant inflammatory macrophage, and neutrophil infiltration, suggesting good histocompatibility and without severe immune reaction.

CONCLUSION

In summary, we have successfully fabricated the heparin-functionalized P(LLA-CL)/heparin composite nanofibers by coaxial electrospinning, and the composite fiber grafts were implanted in the dog model. The morphology observation from SEM indicated that P(LLA-CL) nanofibers and P(LLA-CL)/heparin composite fibers possess smooth surface and with uniformity diameter distribution. The tensile testing results showed good mechanical properties of both P(LLA-CL) and P(LLA-CL)/heparin grafts no matter under dry or wet conditions. Furthermore, the patency rate of P(LLA-CL)/heparin vascular graft could reach 100% in the early period, 50% in the medium term, and 25% in the long term. HE staining indicated that no stenosis of the anastomotic stoma was found after P(LLA-CL)/heparin graft implantation. Therefore, P(LLA-CL)/heparin composite fibrous scaffold could be a better candidate for blood vessel repair.

REFERENCES

1. Lloyd-Jones D, Adams RJ, Brown TM, Carnethon M, Dai S, De Simone G, Ferguson TB, Ford E, Furie K, Gillespie C. Heart disease and stroke statistics—2010 update. Circulation 2010;121: e46–e215.
2. Tiwari A, Cheng KS, Salacinski H, Hamilton G, Seifalian A. Improving the patency of vascular bypass grafts: The role of suture materials and surgical techniques on reducing anastomotic compliance mismatch. Eur J Vascul Endovascul Surg 2003;25: 287–295.
3. Niklason L, Gao J, Abbott W, Hirschi K, Houser S, Marini R, Langer R. Functional arteries grown in vitro. Science 1999;284: 489–493.
4. Mooney D, Mazzoni C, Breuer C, McNamara K, Hern D, Vacanti J, Langer R. Stabilized polyglycolic acid fibre-based tubes for tissue engineering. Biomaterials 1996;17:115–124.
5. Cummings CL, Gawlitta D, Nerem RM, Stegemann JP. Properties of engineered vascular constructs made from collagen, fibrin, and collagen–fibrin mixtures. Biomaterials 2004;25:3699–3706.
6. Shireman PK, Greisler HP. Mitogenicity and release of vascular endothelial growth factor with and without heparin from fibrin glue. J Vascul Surg 2000;31:936–943.
7. Fager G, Hansson GK, Ottosson P, Dahllof B, Bondjers G. Human arterial smooth muscle cells in culture—Effects of platelet-derived growth factor and heparin on growth in vitro. Exp cell Res 1988; 176:319–335.
8. Majack RA, Clowes AW. Inhibition of vascular smooth muscle cell migration by heparin-like glycosaminoglycans. J Cell Physiol 1984;118:253–256.
9. Sarkar S, Sales KM, Hamilton G, Seifalian AM. Addressing thrombogenicity in vascular graft construction. J Biomed Mater Res Part B 2007;82:100–108.
10. Walpoth BH, Bowlin GL. The daunting quest for a small diameter vascular graft. Expert Rev Med Dev 2005;2:647.
11. Shireman PK, Xue L, Maddox E, Burgess WH, Greisler HP. The S130K fibroblast growth factor-1 mutant induces heparin-independent proliferation and is resistant to thrombin degradation in fibrin glue. J Vascul Surg 2000;31:382–390.
12. Edelman ER, Nathan A, Katada M, Gates J, Karnovsky MJ. Perivascular graft heparin delivery using biodegradable polymer wraps. Biomaterials 2000;21:2279–2286.
13. Kwon IK, Matsuda T. Co-electrospun nanofiber fabrics of poly (l-lactide-co-caprolactone) with type I collagen or heparin. Biomacromolecules 2005;6:2096–2105.

14. Chen F, Huang P, Mo X. Electrospinning of heparin encapsulated P (LLA-CL) core/shell nanofibers. Nano Biomed Eng 2010;2:56–60.
15. He C, Xu X, Zhang F, Cao L, Feng W, Wang H, Mo X. Fabrication of fibrinogen/P (LLA-CL) hybrid nanofibrous scaffold for potential soft tissue engineering applications. J Biomed Mater Res Part A 2011;97:339–347.
16. Whang K, Thomas C, Healy K, Nuber G. A novel method to fabricate bioabsorbable scaffolds. Polymer 1995;36:837–842.
17. Larsen G, Spretz R, Velarde-Ortiz R. Templating of inorganic and organic solids with electrospun fibres for the synthesis of large-pore materials with near-cylindrical pores. J Mater Chem 2004;14: 1533–1539.
18. Lee SJ, Yoo JJ, Lim GJ, Atala A, Stitzel J. In vitro evaluation of electrospun nanofiber scaffolds for vascular graft application. J Biomed Mater Res Part A 2007;83:999–1008.
19. Lannutti J, Reneker D, Ma T, Tomasko D, Farson D. Electrospinning for tissue engineering scaffolds. Mater Sci Eng C 2007;27: 504–509.
20. Fukuchi N, Akao M, Sato A. Effect of hydroxyapatite microcrystals on macrophage activity. Biomed Mater Eng 1995;5:219–231.
21. Agrawal C, Ray RB. Biodegradable polymeric scaffolds for musculoskeletal tissue engineering. J Biomed Mater Res 2001;55:141–150.
22. He W, Ma Z, Teo WE, Dong YX, Robless PA, Lim TC, Ramakrishna S. Tubular nanofiber scaffolds for tissue engineered small-diameter vascular grafts. J Biomed Mater Res Part A 2009;90:205–216.
23. Boland ED, Wnek GE, Simpson DG, Pawlowski KJ, Bowlin GL. Tailoring tissue engineering scaffolds using electrostatic processing techniques: A study of poly (glycolic acid) electrospinning. J Macromol Sci Part A 2001;38:1231–1243.
24. Verreck G, Chun I, Rosenblatt J, Peeters J, Dijck AV, Mensch J, Noppe M, Brewster ME. Incorporation of drugs in an amorphous state into electrospun nanofibers composed of a water-insoluble, nonbiodegradable polymer. J Contr Release 2003;92:349–360.
25. Gawaz M, Neumann FJ, Schömig A. Evaluation of platelet membrane glycoproteins in coronary artery disease: Consequences for diagnosis and therapy. Circulation 1999;99:e1–e11.
26. Li WJ, Laurencin CT, Caterson EJ, Tuan RS, Ko FK. Electrospun nanofibrous structure: A novel scaffold for tissue engineering. J Biomed Mater Res 2002;60:613–621.
27. Li WJ, Danielson KG, Alexander PG, Tuan RS. Biological response of chondrocytes cultured in three-dimensional nanofibrous poly (ε-caprolactone) scaffolds. J Biomed Mater Res Part A 2003;67: 1105–1114.
28. Li WJ, Tuli R, Okafor C, Derfoul A, Danielson KG, Hall DJ, Tuan RS. A three-dimensional nanofibrous scaffold for cartilage tissue engineering using human mesenchymal stem cells. Biomaterials 2005;26:599–609.
29. Shields KJ, Beckman MJ, Bowlin GL, Wayne JS. Mechanical properties and cellular proliferation of electrospun collagen type II. Tissue Eng 2004;10:1510–1517.
30. Boland ED, Matthews JA, Pawlowski KJ, Simpson DG, Wnek GE, Bowlin GL. Electrospinning collagen and elastin: Preliminary vascular tissue engineering. Front Biosci 2004;9:C1432.
31. Shin M, Yoshimoto H, Vacanti JP. In vivo bone tissue engineering using mesenchymal stem cells on a novel electrospun nanofibrous scaffold. Tissue Eng 2004;10:33–41.
32. Xu C, Yang F, Wang S, Ramakrishna S. In vitro study of human vascular endothelial cell function on materials with various surface roughness. J Biomed Mater Res Part A 2004;71: 154–161.